

# Robust entanglement of an asymmetric quantum dot molecular system in a Josephson junction

E. Afsaneh<sup>1</sup> and M. Bagheri Harouni<sup>1,2</sup>

<sup>1</sup>*Department of Physics, Faculty of Science, University of Isfahan, Hezar Jerib Str., Isfahan 81746-73441, Iran.*

<sup>2</sup>*Quantum Optics Group, Department of Physics, Faculty of Science, University of Isfahan, Hezar Jerib Str., Isfahan 81746-73441, Iran*

(Dated: June 13, 2019)

We demonstrate how robust entanglement of quantum dot molecular system in a voltage-controlled junction can be generated. To improve the quantum information characteristics of this system, we propose an applicable protocol which contains the implementation of asymmetric quantum dots as well as engineering reservoirs. Quantum dots with tunable energy barriers can provide asymmetric coupling coefficients which can be tuned by gap voltages. Also by engineering reservoirs, superconductors can be used as leads in a biased-voltage junction. The high-controllability characteristics of system supplies the arbitrary entanglement by tuning the controlling parameters. Significantly in concurrence-voltage characteristics, perfect entanglement can be achieved in an asymmetric structure and it can be kept with near-unit magnitude in response to bias voltage increasing.

## I. INTRODUCTION

Recent advancements in condensed matter physics and nanotechnology open new possibilities for the implementation of nanodevices in quantum information studies. Although, the concept of entanglement was basically studied for distinguishable bipartite systems[1–5], in recent years there has been a great deal of interest in quantifying the entanglement of indistinguishable components in condensed matter systems. The elements of these systems are identical massive particles which involve quantum correlations at short distances. The entanglement of indistinguishable particles either bosons or fermions should be characterized with their symmetrized or anti-symmetrized wave functions respectively[6–16].

Particularly, the entanglement of fermions in condensed matter systems can be evaluated by two methods: entanglement of modes[9, 10, 15, 17–19] and entanglement of particles[6–8, 11, 12, 14]. In the former, the entanglement of indistinguishable fermions is associated with the shared modes not particles of subsystems in single particle Hilbert space. But for the latter, the entanglement of fermions specifically is concerned about the antisymmetrization of quantum wave functions of indistinguishable fermionic particles.

For fermionic entanglement of particles approach, firstly the quantum correlations of two fermions in a 2K dimensional single-particle space were characterized[6]. After that more than two indistinguishable particles fermions in higher-dimensional single-particle spaces were analyzed and quantum correlations of pure states in the arbitrary-dimensional Hilbert space were classified[8]. Recently, a multipartite concurrence was introduced for N-indistinguishable fermionic particles in an arbitrary-dimensional pure states[14]. It was presented that the multipartite concurrence can be displayed as an average amount of one observable when two copies of the compound state are accessible.

For studying the entanglement of indistinguishable fermionic particles, quantum dots(QDs)[20, 21] can be taken into account as promising candidates. QDs as one branch of broad two-state qubit systems[22] play prominent roles in nanostructures for their tunable discrete energy levels and also for their easy controllability of barriers by gate voltages.

Also, quantum dot molecules (QDMs) consist of quantum dots which are coupled by tunneling and separated by barriers have received great attention theoretically and experimentally[23–26]. These quantum structures have been selected as the ideal choices for researching the quantum information processing. The analysis of entanglement dynamics between two electrons inside coupled quantum molecules demonstrated the crucial entanglement characteristics[27].

Theoretical [28] and experimental [29] studies showed that asymmetric structure of quantum molecules has enhanced the control of tunneling features. It was theoretically shown that in an asymmetric quantum dot molecular system, the fidelity of entangled photon pairs can be achieved near-unit magnitude[30]. In addition, the asymmetric quantum dot-lead couplings have been extensively implemented in electrical [31] and thermal [32] rectification devices to improve the electric and heat transport technologies.

Moreover, superconducting devices have found impressive interest in quantum information setups [33–35] because of their long intrinsic coherency with no dissipation characteristics. Recent years, employing the superconducting qubits and superconducting resonators have improved the exploring of entanglement [36, 37], teleportation [38–40] and quantum computing [41–43] studies. Superconducting qubits namely phase [44], flux [45, 46] and charge [47, 48] qubits can be connected with microwave [49], electrical [50, 51], mechanical [52] and superconducting [53] resonators. According to the frequency range of superconducting devices, these nanostructures would be driven by microwave [54, 55] or optical [56, 57] fields.

Also, QDs in normal biased-voltage junctions have extensively been used experimentally [58–60] and theoretically [61–63]. Recently, quantum transport through the QDs system in contact with Josephson junctions (JJs) which act as the single transistors to filter the transfer of electrons have attracted a great deal of attention[64–68].

It seems that quantum information studies on an asymmetric quantum dot molecule in a bias-controlled Josephson junction can be considered as an interesting area for research which can provide novel achievements. Therefore in this study, we propose a QDM system in a conventional JJ with asymmetric tunneling coefficients to achieve the robust entanglement and also to keep its magnitude near-unit under the bias voltage control. To this end, we consider the indistinguishable entanglement for our system which becomes possible by evaluating the fermionic concurrence. To explore the quantum information processing of QDM system in a biased-voltage junction, we perform our analysis in Markovian regime. First, we obtain the quantum transport of molecular system to show the current-voltage characteristics (I-V) as one of the important properties of biased-voltage circuits. Then, we investigate the control of the entanglement with respect to bias voltage. We find that with only bias voltage control, the complete controllability to yield perfect entanglement is not possible. Therefore, we apply the strategy of left-right asymmetric coupling strength to achieve the robust entanglement. The dynamics of entanglement and its response to bias voltage in different situations of symmetric and asymmetric couplings demonstrate a wide flexibility of the proposed setup to provide a desired high entanglement. The main advantage of this molecular system includes the feasible controlling elements of easy-tunable bias voltage driving field and the manipulation of quantum dot couplings. Indeed by engineering reservoirs and the presence of superconducting leads, the performance of system is extensively influenced to provide robustly entangled states.

This paper is organized as follows: In Sec.(II), we introduce the proposed model composed of a quantum dot molecular system in a JJ by describing the whole Hamiltonian. We compute the quantum transport of our molecular system in Sec.(III). In Sec.(IV) by introducing symmetric and asymmetric structures, we obtain the entanglement of QDM system under the bias voltage control. In Sec.(V), we present the results of the entanglement behavior in bias voltage changes and its time evolution in constant bias voltages and also for specific order parameters. Finally, we conclude the results in Sec.(VI). In Appendix A, we describe how to diagonalize the Hamiltonian of superconducting leads by applying the Bogoliubov transformation. In Appendix B, we calculate the quantum master equation to study the dynamics of system.

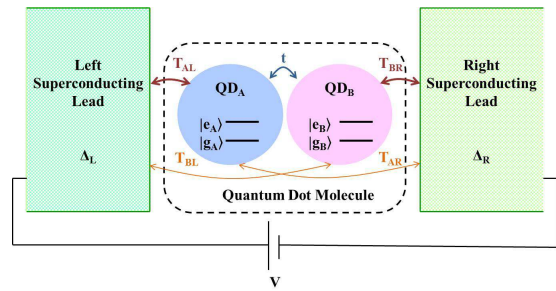


FIG. 1. The proposed physical system: A quantum dot molecule system consists of two coupled quantum dots,  $A$  and  $B$ , with inter-dot coupling strength  $t$  and QD-lead coupling strengths:  $T_{AL}$ ,  $T_{AR}$ ,  $T_{BR}$ ,  $T_{BL}$ . The superconducting leads are under the bias voltage  $V$ .

## II. MODEL

The proposed open quantum system consists of a QDM weakly coupled to the superconducting leads which is demonstrated in Fig.(1), schematically. Applying an external bias voltage between the leads  $L$  and  $R$  induces the electron transport from the left to the right. The Hamiltonian of the whole system can be written as:

$$\hat{H} = \hat{H}_{QDM} + \hat{H}_{Leads} + \hat{H}_{int}, \quad (1)$$

For simplicity, the molecular quantum dot system is taken in spinless Anderson-Holstein model[69, 70]. So,  $\hat{H}_{QDM}$  is expressed as:

$$\hat{H}_{QDM} = \sum_{\alpha} \varepsilon_{\alpha} \hat{d}_{\alpha}^{\dagger} \hat{d}_{\alpha} + t(\hat{d}_A^{\dagger} \hat{d}_B + \hat{d}_A \hat{d}_B^{\dagger}). \quad (2)$$

here,  $\hat{H}_{QDM}$  introduces the spinless double quantum dot(DQD) with electronic energy levels  $\varepsilon_{\alpha}$  for  $\alpha = A, B$ . Beyond the Coulomb blockade regime, each QD is considered in single electron conditions[71, 72]. In the second term,  $t$  describes the inter-dot hopping strength which can be tuned using an applied gate voltage. In Eq.(1),  $\hat{H}_{Leads}$  corresponds to the left and right superconducting leads which are described by the mean-field Hamiltonian as [73, 74]:

$$\hat{H}_{Leads}^{MF} = \sum_{k\nu\sigma} \xi_{k\nu} \hat{c}_{k\nu\sigma}^{\dagger} \hat{c}_{k\nu\sigma} + \sum_{k\nu} \left( \Delta_{\nu} \hat{c}_{k\nu\uparrow}^{\dagger} \hat{c}_{-k\nu\downarrow}^{\dagger} + \Delta_{\nu}^* \hat{c}_{-k\nu\downarrow} \hat{c}_{k\nu\uparrow} \right). \quad (3)$$

Here,  $\hat{c}_{k\nu\sigma}^{\dagger}$  ( $\hat{c}_{k\nu\sigma}$ ) is the creation (annihilation) operator of an electron with momentum  $k$  and spin  $\sigma = \uparrow, \downarrow$  in lead  $\nu = L, R$ . In this relation,  $\xi_{k\nu} = \varepsilon_k - \mu_{\nu}$  is the particle energy in which  $\varepsilon_k$  denotes the single-particle energy regards to the electrochemical potential  $\mu_{\nu}$ . Moreover,  $\Delta_{\nu} = |\Delta_{\nu}| e^{i\phi_{\nu}}$  remarks the superconducting energy gap of lead  $\nu$  with the superconducting phase,  $\phi_{\nu}$ . The mean field Hamiltonian could be diagonalized by applying Bogoliubov transformation to obtain (Appendix A):

$$\hat{H}_{Leads} = E_G + \sum_{k\nu\sigma} E_{\nu k} \hat{\gamma}_{k\nu\sigma}^{\dagger} \hat{\gamma}_{k\nu\sigma}, \quad (4)$$

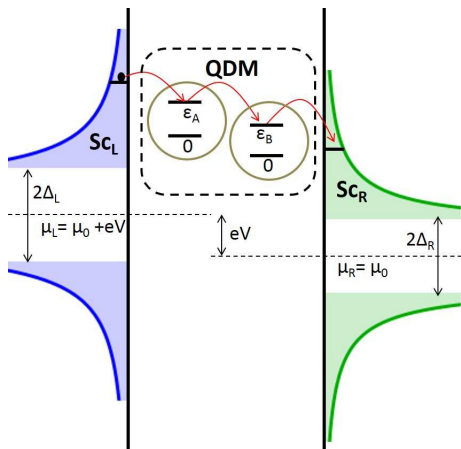


FIG. 2. The density of states in the superconducting reservoirs of  $Sc_L/QDM/Sc_R$  junction. The asymmetric applied bias voltage lets carriers to flow from the left reservoir to the QDM and then to the right lead.

where  $E_G$ , the ground state energy, represents the Cooper pair condensate energy. The interaction Hamiltonian,  $\hat{H}_{int}$  in Eq.(1), corresponds to the tunneling between the QDs and electrodes which can be written as:

$$\hat{H}_{int} = \sum_{k\nu\alpha} \left( T_{k\nu\alpha} \hat{c}_{k\nu}^\dagger \hat{d}_\alpha + T_{k\nu\alpha}^* \hat{c}_{k\nu} \hat{d}_\alpha^\dagger \right). \quad (5)$$

The tunneling coefficient,  $T_{k\nu\alpha}$ , describes the coupling strength depending on  $k$ , the momentum of an electron in lead  $\nu$ , the site of quantum dot  $\alpha$ .

To investigate the time evolution of system, firstly the quantum master equation(QME) and the density matrix are obtained (Appendix B) and then we calculate the current and entanglement in the following sections.

### III. CURRENT

In order to have transport through the present system(Fig. (1)), the asymmetric bias voltage is applied to the electrodes which is shown in Fig. (2). External bias voltage changes the density of states such that the electrochemical energy level of the left lead is shifted higher than the energy levels of the QDM and the right lead which causes flowing current through the junction.

Current as a measurable quantity denotes the variation of particle number,  $N$ , in lead  $\nu$  which is defined as[75]:

$$\begin{aligned} \hat{I}_\nu(t) &= -e \frac{d\hat{N}_\nu}{dt} = \frac{ie}{\hbar} [\hat{N}_\nu(t), \hat{H}_I(t)] \\ &= \frac{ie}{\hbar} \sum_{k\alpha} (T_{k\alpha} \hat{c}_{k\nu}^\dagger \hat{d}_\alpha - T_{k\alpha}^* \hat{c}_{k\nu} \hat{d}_\alpha^\dagger), \end{aligned} \quad (6)$$

where  $\hat{N}_\nu = \sum_\nu \hat{c}_\nu^\dagger \hat{c}_\nu$ . According to the QME formalism, Eq.(20), the density matrix evolution of the system would be written as  $\dot{\hat{\rho}} = \hat{M}\hat{\rho}$ . In this relation matrix  $\hat{M}$  shows

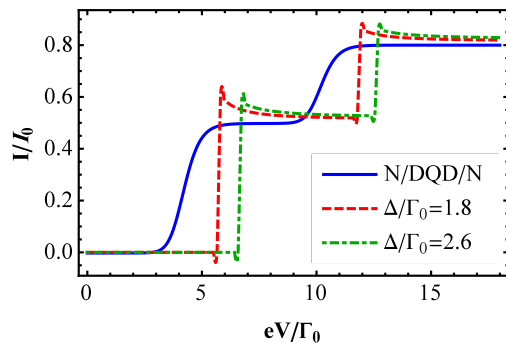


FIG. 3. Current-voltage characteristics in specific superconducting energy gaps. Normal leads: Solid line  $\Delta = 0$ , Superconducting leads: Dashed line  $\frac{\Delta}{\Gamma_0} = 1.8$ , Dotted  $\frac{\Delta}{\Gamma_0} = 2.6$  when  $\Gamma_0 = \pi N_F |T|^2$ ,  $I_0 = e \frac{\Gamma_0}{\hbar}$  and  $\Delta_L = \Delta_R = \Delta$ .

the properties of master equation. Therefore, we can rewrite the current formula, Eq.(6), as [68, 76]:

$$\hat{I}_\nu(t) = \frac{e}{\hbar} \langle \hat{N} | \hat{M}_\nu | \hat{\rho}(t) \rangle, \quad (7)$$

where  $\hat{M}_\nu$  shows the contribution of lead  $\nu$  in matrix  $\hat{M}$ . In steady state of the system, by taking so long time ( $t \rightarrow \infty$ ), the stationary transport is shown in Fig.(3) containing the plots of normal junction ( $\Delta = 0$ ) and JJ with different energy gaps.

According to I-V characteristics which is shown in Fig.(3), the magnitude of current is growing by the increase of bias voltage. Only in energies equal to the quantum dots' energy levels, the current hits the peaks in delta type for the superconducting leads while it illustrates the smooth steps for the normal leads. Although, the current level of system is increased by rising the magnitude of energy gaps, it reaches the platform for the large enough bias voltage.

In all calculations in order to deal with only the quasi-particle transport and ignoring the Cooper pair current, we assume all energy levels are far enough from the order parameter of leads.

### IV. CONCURRENCE

It is convenient to apply the concurrence as a measure of entanglement for two qubit systems. In the following, first this measure of entanglement for two distinguishable qubits is defined. Then, fermionic concurrence for indistinguishable particles will be characterized and evaluated in analogue with Wootters' formula.

#### A. Concurrence of distinguishable particles

For the first time, Wootters introduced the measure of concurrence to evaluate the entanglement of qubits with

two parties in both pure and mixed states [77, 78]. This measure of entanglement is defined as:

$$C(\rho) = \text{Max}[0, \lambda_1 - \lambda_2 - \lambda_3 - \lambda_4], \quad (8)$$

in which,  $\lambda_i$ , ( $i = 1, 2, 3, 4$ ) represents the non-negative eigenvalues of a matrix  $\hat{R}$  in decreasing order  $\lambda_1 > \lambda_2 > \lambda_3 > \lambda_4$ . The matrix  $\hat{R}$  is defined as:

$$\hat{R} = \sqrt{\sqrt{\hat{\rho}}\hat{\rho}\sqrt{\hat{\rho}}}, \quad (9)$$

where  $\hat{\rho} = \sum_i p_i |\psi_i\rangle\langle\psi_i|$  denotes the density matrix of system in which,  $p_i$  is the probability of each state of decompositions. Also  $\hat{\rho} = (\hat{\sigma}_y \otimes \hat{\sigma}_y)\hat{\rho}^*(\hat{\sigma}_y \otimes \hat{\sigma}_y)$ . In this relation,  $\hat{\sigma}_y$  describes the  $y$  element of Pauli matrices and  $\hat{\rho}^*$  represents the complex conjugate of the density matrix.

### B. Concurrence of indistinguishable fermions

In condensed matter systems, the entanglement of electrons should be taken into account as indistinguishable particles. To characterize the entanglement of indistinguishable fermions, the simplest possible system with the lowest-dimensional situation is defined for two fermions in four-dimensional single-particle Hilbert space which is generally in a six-dimensional two-particle space[8]. An arbitrary state of two fermions is given:

$$|\psi\rangle = \sum_{i,j=1}^4 \psi_{i,j} \hat{c}_i^\dagger \hat{c}_j^\dagger |0\rangle \quad (10)$$

where  $\psi_{ij}$  indicates the coefficient matrix. Its dual matrix  $\tilde{\psi}_{ij} = \frac{1}{2} \sum_{k,l=1}^4 \varepsilon^{i,j,k,l} \psi_{k,l}^*$  is defined with antisymmetric unit tensor  $\varepsilon^{i,j,k,l}$ . In this case, fermionic concurrence in analogy with distinguishable two-qubit concurrence Eq.(8) can be written as[6–8, 13, 14]:

$$\begin{aligned} C_F(|\psi\rangle) &= |\langle\tilde{\psi}|\psi\rangle| = \left| \sum_{i,j,k,l=1}^4 \varepsilon^{i,j,k,l} \psi_{i,j} \psi_{k,l} \right| \\ &= 8|\psi_{12}\psi_{34} + \psi_{13}\psi_{42} + \psi_{14}\psi_{23}| \end{aligned} \quad (11)$$

Also, this relation can be expressed as[14, 79]:

$$C_F(|\psi\rangle) = \sqrt{2(1 - 2\text{Tr}[\hat{\rho}^2])} \quad (12)$$

in which  $\hat{\rho}$  denotes the single-fermion reduced density matrix. This means that the Wootters formula Eq.(8) which states concurrence was proved completely for two indistinguishable fermions.

### C. Concurrence in our system

Due to the role of electrons in construction of QDs as qubits, quantum dots are involved in fermionic statistics

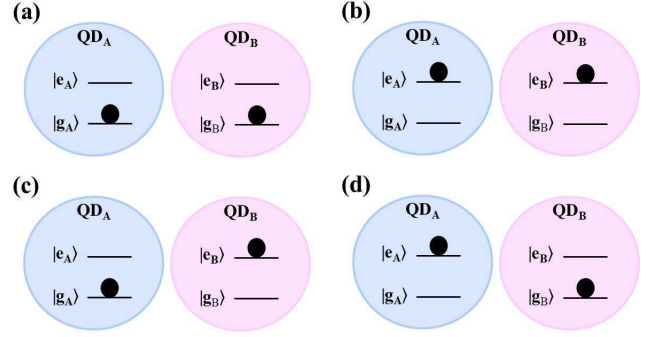


FIG. 4. Configuration of initial states of two spinless electrons of molecular double quantum dot

as well as antisymmetric wave functions. Therefore to calculate the entanglement of coupled QDs, it is needed to use the entanglement of indistinguishable particles method. In our study, it is assumed that quantum dots with spinless electrons can be realized as qubits by their orbital electronic degrees of freedom in quantum information theory. These two spinless electrons in a double-well potential are close enough to each other in short distance to have quantum correlations. Therefore, they can treat as indistinguishable particles entanglement.

Our proposed molecular system is occupied with total two spinless electrons in four-dimensional single-particle Hilbert space. The two-particle states of system can be written as  $|\psi\rangle_{AB} = |\Phi\rangle_A \otimes |\Phi\rangle_B$ , in which  $|\Phi\rangle_A$  ( $|\Phi\rangle_B$ ) shows the state of qubit A(B). As each electron of each dot can capture either ground or excited state, the general form of occupation states can be represented as  $|g_A, e_A, g_B, e_B\rangle = |g_A, e_A\rangle \otimes |g_B, e_B\rangle$ . Fig.(4) shows the configuration of all possible initial states of our two-spinless electron system.

Here, we discuss about the influence of energy-dependent coefficients on the entanglement of quantum dot molecular system. The energy contributions which can be taken into account asymmetrically originated from the QD-reservoir couplings. Indeed, the unequal left and right superconducting energy gaps of reservoirs ( $\Delta_L \neq \Delta_R$ ) can intensively influence the behavior of entanglement. According to Eq.(20) and Eq.(21) the energy-dependent of molecular system is affected by a set of elements: distribution function, density of states and coupling coefficients. To observe the prominent role of asymmetry on the entanglement of QDM system, we consider the coupling coefficients and superconducting energy gaps in right-left asymmetric situation. For this purpose, the strength of coupling coefficients which strongly depends on the properties of QDs can easily be tuned left-right asymmetrically by mean of the relevant gap voltages. Also, the superconducting energy gaps of left and right reservoirs can be simply chosen unequally in the arrangement of setup. To present the effect of asymmetric coupling coefficients, we define the asymmetric factor as

a function of coupling contributions:

$$\kappa = \frac{\kappa_A + \kappa_B}{2} \quad (13)$$

in which  $\kappa_\alpha = \left| \frac{T_{\alpha L} - T_{\alpha R}}{T_{\alpha L} + T_{\alpha R}} \right|$ ,  $\alpha = A, B$ . Here,  $T_{AL}$  denotes the coupling of  $QD_A$  to the near-lead(Left Lead) and  $T_{AR}$  shows the coupling of this  $QD$  to the far-lead(Right Lead). Similarly, the coupling of  $QD_B$  with the far-lead(Left Lead) is shown by  $T_{BL}$  and with the near-lead(Right Lead) is indicated by  $T_{BR}$  which is illustrated in Fig.(1). All these coupling parameters are considered positive which provide the magnitude of asymmetric factor from zero to unit.

Mostly, in the study of QDs system for simplification, the coupling of QD with the far-lead is ignored[80]. However, we assume the both coupling of each QD to the near-lead and far-lead non-zero with only different strengths which are involved in the asymmetric factor definition, (Eq.(13)).

According to the definition of asymmetric factor, (Eq.(13)) and also refer to the configuration of the initial states(Fig.(4)), we investigate the entanglement of our proposed quantum dot molecular system in two parts, namely symmetric and asymmetric structures as follows.

#### D. Symmetric Structure

The initial state of symmetric structure is defined as the superposition of states in (c) or (d) configurations in Fig.(4) which can provide Bell states. Particularly, we use the state  $\frac{1}{2}(|1, 0, 0, 1\rangle - |0, 1, 1, 0\rangle)$  for the symmetric structure.

Also, in this structure, the left coupling coefficient of each QD is similar to the right one ( $T_{AL} = T_{AR}$  and  $T_{BL} = T_{BR}$ ) which means the left-right symmetric coupling coefficients. This situation supplies the minimum magnitude of the asymmetric factor,  $\kappa = 0$ . Also, this situation corresponds to equal superconducting energy gaps of the left and right reservoirs ( $\Delta_L = \Delta_R$ ). In these conditions, the entanglement of QDM system is obtained only for the initial entangled states.

For this purpose, we consider the following Bell state as an initial state with the highest degree of entanglement:

$$\rho(0) = \begin{bmatrix} 0 & 0 & 0 & 0 \\ 0 & 0.5 & -0.5i & 0 \\ 0 & 0.5i & 0.5 & 0 \\ 0 & 0 & 0 & 0 \end{bmatrix}. \quad (14)$$

#### E. Asymmetric Structure

The configuration of asymmetric structure can involves in one of (a) or (b) in Fig.( 4) that we choose (a) configuration. This situation means that both QDs are occupied with spinless electrons in ground states of each QD.

Moreover, the asymmetric structure is defined for the left-right different coupling coefficients with  $0 < \kappa \leq 1$  magnitude and the unequal order parameters of reservoirs,  $\Delta_L \neq \Delta_R$ . In this group, the ideal asymmetry element is achieved for the maximum amount of asymmetric factor  $\kappa \simeq 1$ . The situation of ideal asymmetry is available when one of the left or right coupling coefficient is much larger than the other one. To apply the ideal asymmetry properties in physically rational considerations, we assume that each QD is coupled to the near-lead with much larger strength than the far-lead. In other words, we consider  $\Gamma_{AL} \gg \Gamma_{AR}$  and  $\Gamma_{BR} \gg \Gamma_{BL}$  to realize the most magnitude of asymmetric factor. An interesting feature in the composed systems is the realization of entanglement from the initial unentangled states. This important point would be accomplished in the asymmetric structure. To investigate this significant situation in the present system, we assume an appropriate separated initial state as:

$$\rho(0) = \begin{bmatrix} 1 & 0 & 0 & 0 \\ 0 & 0 & 0 & 0 \\ 0 & 0 & 0 & 0 \\ 0 & 0 & 0 & 0 \end{bmatrix}. \quad (15)$$

In the next section, we present the concurrence behavior of the present QDM system for both symmetric and asymmetric structures.

## V. RESULTS

In this section, we investigate the concurrence behavior of molecular system firstly in response to bias voltage, secondly by the time evolution in constant voltage and finally through the dynamics for specific superconducting energy gaps.

#### A. Concurrence-Voltage characteristics

The concurrence-voltage (C-V) characteristics demonstrates the response of concurrence to the bias voltage as an external easy-tunable driving field. Fig.(5) shows C-V characteristics for normal reservoirs with  $\Delta = 0$  and superconducting ones with specific order parameters in the conditions of symmetric structure (Panel(a)) and asymmetric one (Panel(b)). In panel (a) of Fig.(5), the concurrence shows degradation for the symmetric structure while in panel (b) of this figure, the concurrence indicates rising for the asymmetric conditions in higher values of bias voltage. In both panels of Fig.(5), the concurrence changes in the energy levels of QDs with the step shapes for the normal leads and with the delta peaks for the superconducting reservoirs. The presence of superconductors as reservoirs provides stronger response than the normal leads. This effect is obvious in Fig.(5) when in panel (a) the concurrence is decreased with higher values of potential and in panel (b) concurrence shows increment

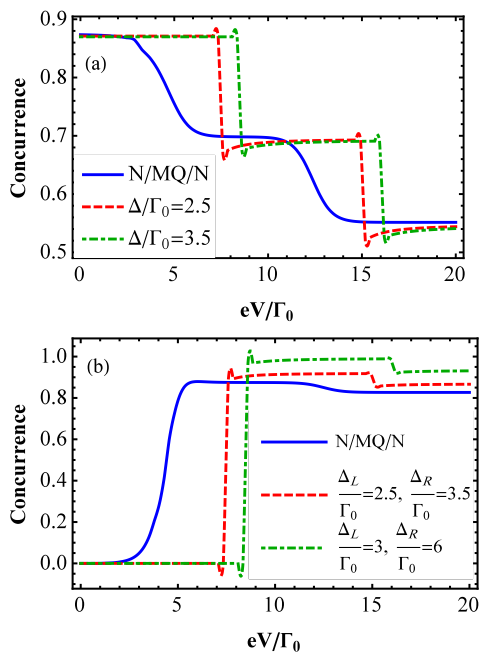


FIG. 5. The concurrence-voltage characteristics for the symmetric structure in panel (a) and for the asymmetric structure in panel (b). Normal leads: Solid line  $\Delta = 0$ , Superconducting leads: panel (a), Dashed line  $\frac{\Delta}{\Gamma_0} = 2.5$ , Dotted-dashed  $\frac{\Delta}{\Gamma_0} = 3.5$  ( $\Delta_L = \Delta_R = \Delta$ ) and panel (b), Dashed line  $\frac{\Delta_L}{\Gamma_0} = 2.5$ ,  $\frac{\Delta_R}{\Gamma_0} = 3.5$ ; Dotted-dashed  $\frac{\Delta_L}{\Gamma_0} = 3$ ,  $\frac{\Delta_R}{\Gamma_0} = 6$ .  $\Gamma_0 = \pi N_F |T|^2$ .

in higher magnitude for the Josephson junction than the normal one. Also, the influence of superconducting reservoirs is displayed more clearly when by increasing the amount of superconducting energy gaps, the concurrence has lower magnitude for the symmetric structure (panel (a)) and inversely for the asymmetric group (panel (b)).

It is interesting that our proposed setup is able to support two different fundamental concepts of physics which are quantum transport and quantum entanglement simultaneously in response to bias voltage changes. There are two different responses to the increase of bias voltage in I-V characteristics (Fig.(3)) and C-V one (Fig.(5)-(a)) which are increasing for the former and decreasing for the later in the symmetric structure. This various behavior can be interpreted as the response of electrons to the external bias voltage. As a consequence of the bias voltage increasing, electrons are accelerated which cause a rising current across the symmetric junction. This faster movement of carriers means that the electrons with the initial entangled states (Eq.(14)) in the symmetric coupling situation can be present in a shorter period of time which leads to have less time to be entangled. Therefore, the entanglement degradation in response to bias voltage rising does make sense for the left-right symmetric conditions.

The behavior of concurrence originates from the mov-

ing manner of electrons. So, it would be physically reasonable that carriers can move more quickly through the Josephson junction than the normal one which means the lower value of entanglement in JJ for the left-right symmetric situation. However, the electrons of asymmetric structure with the initial unentangled states (Eq.(15)) have different conditions. The asymmetric coupling coefficients provide a bounded-like situation for the unentangled electrons which give them an opportunity to be well entangled. It means that although electrons can move faster by the increase of bias voltage, the left-right asymmetric situation arranges the possibility of being robustly entangled for them. Therefore, it would be logical that C-V characteristics shows increasing in response to bias voltage rising for asymmetric group.

It is a crucial point that although the concurrence of asymmetric structure (panel (b) of Fig.(5)) behaves differently from the symmetric one (panel (a) of Fig.(5)), their origins are the same. The main reason for this variety behavior of concurrence refers to the powerful strength of our proposed setup in controlling the features to obtain the desired results. In addition, the quantum correlation between the localized sites (QDs) is under investigation for the present system. This correlation is attributed to the presence of electron in each QD. In a higher current magnitude, the electrons are passed faster through the QDM system and consequently, the correlation between localized sites is decreased.

## B. Dynamics of concurrence in constant bias voltage

The time evolution of concurrence for given values of superconducting energy gap in a constant bias voltage is demonstrated for symmetric and asymmetric structures in panels (a) and (b) of Fig.(6), respectively. According to Eq.(14) and Eq.(15) which express the initial states of symmetric and asymmetric group conditions, the concurrence of these structures are increased and decreased through the time, respectively. In Fig.(6), the concurrence of both left-right symmetric and asymmetric situations decay faster for JJs than the normal ones to receive the ultimate magnitudes only with opposite manner. Indeed, the decay rate of concurrence is speeded up by increasing the superconducting energy gap for them.

## C. Dynamics of concurrence for specific superconducting energy gaps

Fig.(7) indicates the time evolution of entanglement for energies which are in resonant with the energy levels of QDs,  $eV = \varepsilon_i + \Delta$  ( $i = A, B$ ), in symmetric structure (panel (a)) and asymmetric one (panel (b)). These resonant points are illustrated as peaks with respect to bias voltage in Fig.(5). Due to the proximity effect of superconducting reservoirs, the concurrence be-

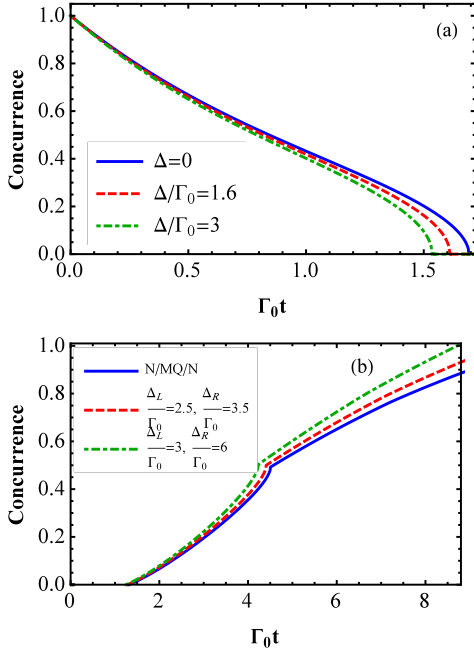


FIG. 6. The dynamics of concurrence for the symmetric structure with constant low bias voltage in panel (a) and for the asymmetric structure with constant high bias voltage in panel (b). Normal leads: Solid line  $\Delta = 0$ , Superconducting leads: panel (a), Dashed line  $\frac{\Delta}{\Gamma_0} = 1.6$ , Dotted-dashed  $\frac{\Delta}{\Gamma_0} = 3$  ( $\Delta_L = \Delta_R = \Delta$ ) and panel (b), Dashed line  $\frac{\Delta_L}{\Gamma_0} = 2.5$ ,  $\frac{\Delta_R}{\Gamma_0} = 3.5$ ; Dotted-dashed  $\frac{\Delta_L}{\Gamma_0} = 3$ ,  $\frac{\Delta_R}{\Gamma_0} = 6$ .  $\Gamma_0 = \pi N_F |T|^2$ .

has differently in two sides of each resonant points. For the left-right symmetric group, concurrence shows longer elapsed time for the left side of the resonant point ( $eV = \varepsilon_i + \Delta - 0.01; i = A, B; \Delta_L = \Delta_R = \Delta$ ) than the right side ( $eV = \varepsilon_i + \Delta + 0.01$ ) which is illustrated in panel (a) of Fig.(7). However for high bias voltage  $eV \gg 0$ , the dynamics of concurrence decays in moderate rate. For asymmetric situation which is shown in panel (b) of Fig.(7), the time evolution of concurrence for the first resonant point ( $eV = \varepsilon_A + \Delta_L$ ) which corresponds to the low bias voltage shows different behavior than the second one ( $eV = \varepsilon_B + \Delta_R$ ).

The dynamics of concurrence for the left side of the first resonant point ( $eV = \varepsilon_A - \Delta_L - 0.01$ ) illustrates no response through time and also it shows the longest decay rate for the right side of this point ( $eV = \varepsilon_A + \Delta_L + 0.01$ ). This behavior means that for asymmetric situation, the amount of bias voltage plays more important role than the other elements in the concurrence time evolution. However for the second resonant point with larger bias voltage, the dynamics of concurrence is similar to the symmetric situation (panel (a) of Fig.(7)) only with inverse manner of decay. In other words, the dynamics of concurrence shows longer elapsed time for the right side of the second resonant point,  $eV = \varepsilon_B + \Delta_R + 0.01$ , than the left side,  $eV = \varepsilon_B + \Delta_R - 0.01$ . Also for high bias

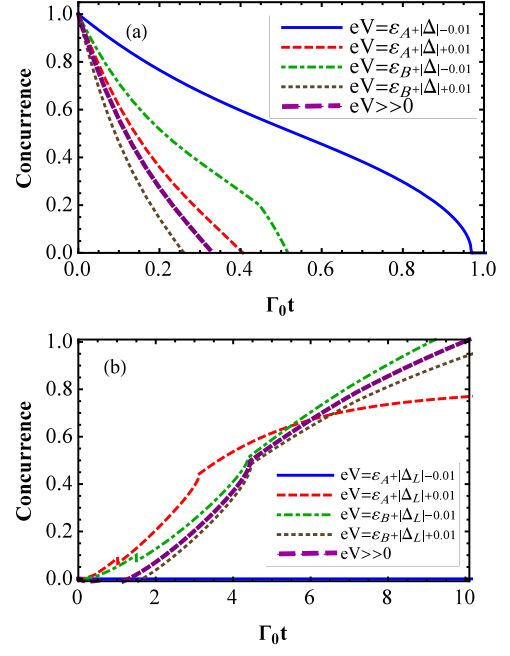


FIG. 7. The dynamics of concurrence for bias voltages in resonant with QD's energy levels, panel (a): for the symmetric structure and panel (b) for the asymmetric structure. Solid line: left side of the first resonant point, Dashed line: right side of the first resonant point, Dot-dashed line: left side of the second resonant point, Dotted line: right side of the second resonant point and Thick-dashed line: high bias.  $\Gamma_0 = \pi N_F |T|^2$  (for panel (a)  $\Delta_L = \Delta_R = \Delta$ ).

voltage  $eV \gg 0$ , it decays in moderately rate.

## VI. CONCLUSION

In summary, we proposed a protocol to obtain perfect entanglement for two coupled QDs molecular structure in a voltage-controlled junction. In this strategy, we focused on the arrangement of different controlling elements to enhance the quantum information characteristics of system. First by engineering the reservoirs, we applied superconductors as leads using the significant properties of Josephson junction under the bias voltage control. Second, we utilize the energy couplings of QD-reservoirs asymmetrically. The main advantage of this hybrid quantum system refers to its wide strength of controllability due to the easy tuning driven bias voltage and also control of coupling coefficients by manipulating the quantum dot barriers with respect to the required results. In concurrence-voltage characteristics, applying the asymmetric coupling energy conditions can provide high degree of entanglement while for the symmetric situation, entanglement shows degradation.

## APPENDIX A: DIAGONALIZING THE HAMILTONIAN OF SUPERCONDUCTING LEADS

It would be possible to diagonalize the superconducting Hamiltonian. The mean-field Hamiltonian of superconducting leads is mostly diagonalized by Bogoliubov transformation. To this end, we consider the following Bogoliubov transformation [81]:

$$\begin{aligned}\hat{c}_{-k\nu\downarrow} &= u_{k\nu}\hat{\gamma}_{-k\nu\downarrow} - v_{k\nu}^*\hat{\gamma}_{k\nu\uparrow}^\dagger, \\ \hat{c}_{k\nu\uparrow}^\dagger &= u_{k\nu}^*\hat{\gamma}_{k\nu\uparrow}^\dagger + v_{k\nu}\hat{\gamma}_{-k\nu\downarrow},\end{aligned}\quad (16)$$

where  $\hat{\gamma}_{k\nu\sigma}^\dagger$  ( $\hat{\gamma}_{k\nu\sigma}$ ) denotes the creation (annihilation) operator of Bogoliubov fermionic quasiparticle excitation. Bogoliubov quasiparticles follow the fermionic anticommutation relation  $\{\hat{\gamma}_{k\nu\sigma}, \hat{\gamma}_{k'\nu'\sigma'}^\dagger\} = \delta_{\nu\nu'}\delta_{kk'}\delta_{\sigma\sigma'}$ . The complex number parameters  $u_{k\nu}$  and  $v_{k\nu}$  adopting the relation  $|u_{k\nu}|^2 + |v_{k\nu}|^2 = 1$  are defined as:

$$\begin{aligned}u_{k\nu} &= e^{-i\Phi_\nu} \sqrt{\frac{1}{2} \left( 1 + \frac{\xi_{k\nu}}{|E_{\nu k}|} \right)}, \\ v_{k\nu} &= \sqrt{\frac{1}{2} \left( 1 - \frac{\xi_{\nu k}}{|E_{k\nu}|} \right)}.\end{aligned}\quad (17)$$

Here,  $E_{\nu k} = \sqrt{\xi_{k\nu}^2 + |\Delta_\nu|^2}$  indicates the quasiparticle energy. Inserting the Bogoliubov transformation (16) into the mean-field Hamiltonian (3), the diagonalized Hamiltonian is achieved:

$$\hat{H}_{Leads} = E_G + \sum_{k\nu\sigma} E_{\nu k} \hat{\gamma}_{k\nu\sigma}^\dagger \hat{\gamma}_{k\nu\sigma}, \quad (18)$$

in which the ground state energy  $E_G$  shows the Cooper pair condensate energy.

## APPENDIX B: DYNAMICS OF SYSTEM

To study the dynamics of system, we start from the Liouville-von Neumann equation of the complete system in the interaction picture [82]. A comparison between the characteristics time scales of the system, the QD relaxation time and the superconducting coherence time as the environment time scale, implies that the present system would be studied under the Markovian approximation [67, 83, 84]. After partial tracing out the lead degrees of freedom and applying the Born-Markov approximation, the quantum master equation (QME) for the reduced density matrix is obtained:

$$\begin{aligned}\frac{d\hat{\rho}(t)}{dt} &= -\frac{i}{\hbar}[\hat{H}_I, \hat{\rho}(t)] \\ &\quad - \frac{1}{\hbar^2} \int_0^\infty dt' Tr_B \{ [\hat{H}_I(t), [\hat{H}_I(t'), \hat{\rho}(t)]] \},\end{aligned}\quad (19)$$

where  $\hat{\rho}$  denotes the reduced density matrix of system in the interaction picture. The first term shows the Lamb

shift which is ignored in the present study and the second one represents the dissipation of system.

In general case, the interaction Hamiltonian can be considered as  $\hat{H}_I = \sum_\alpha \hat{A}_\alpha \hat{B}_\alpha$  with the operators  $\hat{A}_\alpha$  and  $\hat{B}_\alpha$  which satisfy the commutation relation  $[A_\alpha, B_\alpha] = 0$  and act on the system and leads Hilbert spaces, respectively. Finally, the master equation for the central system of QDM in the presence of superconducting leads is derived as:

$$\begin{aligned}\frac{d\hat{\rho}_s(t)}{dt} &= \frac{1}{\hbar^2} \sum_\omega \sum_{\alpha,\beta} \left( \Gamma_{\alpha,\beta}^-(\omega) \left( \hat{A}_\beta(\omega) \hat{\rho}_s(t) \hat{A}_\alpha^\dagger(\omega) \right. \right. \\ &\quad \left. \left. - \frac{1}{2} \{ \hat{A}_\alpha^\dagger(\omega) \hat{A}_\beta(\omega), \hat{\rho}_s(t) \} \right) \right. \\ &\quad \left. + \Gamma_{\alpha,\beta}^+(\omega) \left( \hat{A}_\alpha^\dagger(\omega) \hat{\rho}_s(t) \hat{A}_\beta(\omega) \right. \right. \\ &\quad \left. \left. - \frac{1}{2} \{ \hat{A}_\beta(\omega) \hat{A}_\alpha^\dagger(\omega), \hat{\rho}_s(t) \} \right) \right),\end{aligned}\quad (20)$$

where  $\{\}$  denotes the anticommutation relation. The dissipation coefficients  $\Gamma_{\alpha,\beta}^-(\omega) = \int_0^\infty ds e^{i\omega s} \langle \hat{B}_\alpha(t) \hat{B}_\beta^\dagger(t-s) \rangle_B$  and  $\Gamma_{\alpha,\beta}^+(\omega) = \int_0^\infty ds e^{i\omega s} \langle \hat{B}_\beta^\dagger(t) \hat{B}_\alpha(t-s) \rangle_B$  are related to the bath correlation function. For superconducting leads, the distribution function is defined as  $\langle \hat{\gamma}_{k,\nu}^\dagger \hat{\gamma}_{k,\nu} \rangle_B = \frac{1}{e^{\beta E_{k,\nu}} + 1} = f^+(E_{k,\nu})$  and also  $\langle \hat{\gamma}_{k,\nu} \hat{\gamma}_{k,\nu}^\dagger \rangle_B = (1 - f^+(E_{k,\nu})) = f^-(E_{k,\nu})$ . So, we have

$$\begin{aligned}\Gamma_{\alpha,\beta}^+(\omega) &= 2\pi \sum_{k\nu\sigma} T_{k\nu\alpha} T_{k'\nu'\beta}^* \langle \hat{\gamma}_{k\nu\sigma}^\dagger \hat{\gamma}_{k'\nu'\sigma'} \rangle \\ &= 2\pi |T_{k\nu\alpha}|^2 \int dE f^+(E_{k,\nu}) R_{k\nu}(E_{k\nu}), \\ \Gamma_{\alpha,\beta}^-(\omega) &= 2\pi \sum_{k\nu\sigma} T_{k\nu\alpha} T_{k'\nu'\beta}^* \langle \hat{\gamma}_{k\nu\sigma} \hat{\gamma}_{k'\nu'\sigma'}^\dagger \rangle_B \\ &= 2\pi |T_{k\nu\alpha}|^2 \int dE f^-(E_{k,\nu}) R_{k\nu}(E_{k\nu}).\end{aligned}\quad (21)$$

According to the BCS theory, the superconducting density of states  $R_\nu(E)$  is defined [66–68]:

$$R_{k\nu}(E) = N_F \frac{|E_{k\nu}|}{\sqrt{E_{k\nu}^2 - |\Delta_\nu|^2}}, \quad (22)$$

in which  $N_F$  denotes the density of states for normal reservoirs which is assumed as a constant parameter close to the Fermi level of energy. We define  $\Gamma_0 = 2\pi N_F |T_{k\nu\alpha}|^2$  so, Eq.(21) can be written as:

$$\begin{aligned}\Gamma_{\alpha,\beta}^+(\omega) &= \Gamma_0 \int dE f^+(E_{k,\nu}) \frac{|E_{k\nu}|}{\sqrt{E_{k\nu}^2 - |\Delta_\nu|^2}}, \\ \Gamma_{\alpha,\beta}^-(\omega) &= \Gamma_0 \int dE f^-(E_{k,\nu}) \frac{|E_{k\nu}|}{\sqrt{E_{k\nu}^2 - |\Delta_\nu|^2}}.\end{aligned}\quad (23)$$

To parameterize the effect of left-right asymmetric coefficients in Eq.(23), we define  $T_{k\nu\alpha} = \gamma_{\alpha,\nu} T_0$  in which  $\gamma_{\alpha,\nu}$  ( $\nu = L, R$ ,  $\alpha = A, B$ ) denotes the asymmetric constant parameter and  $T_0$  shows the symmetric coupling coefficient.

In Eq.(20)  $\hat{A}_\alpha(\omega)$  denotes the projection super-operator which acts on the eigenoperator of system with eigenvalue of  $\omega$ . Here, as we encounter with a bipartite central system, we introduce the eigenoperator as  $|\omega\rangle = |\varepsilon_A, \varepsilon_B\rangle = |\varepsilon_A\rangle_A \otimes |\varepsilon_B\rangle_B$  with eigenvalue  $\omega = \{\omega_A, \omega_B\}$ . Therefore, we define the super-operator:

$$\hat{A}(\omega) = \hat{A}(\omega_i, \omega_j) = \sum_{\substack{\omega_i = \varepsilon'_i - \varepsilon_i \\ \omega_j = \varepsilon_j - \varepsilon_j}} |\varepsilon_i \varepsilon_j\rangle \langle \varepsilon_i \varepsilon_j | \hat{A} | \varepsilon'_i \varepsilon'_j \rangle \langle \varepsilon'_i \varepsilon'_j |. \quad (24)$$

The computational basis which is applied for the present

system includes  $|1\rangle = |g_A, g_B\rangle$ ,  $|2\rangle = |g_A, e_B\rangle$ ,  $|3\rangle = |e_A, g_B\rangle$  and  $|4\rangle = |e_A, e_B\rangle$  where  $|g_\alpha\rangle$  and  $|e_\alpha\rangle$  represent the ground and excited states of quantum dots respectively ( $\alpha = A, B$ ).

To consider the weak-coupling regime, the energies of system should be under the relation of  $\Gamma_{\alpha,\beta}^\pm < \varepsilon_A, \varepsilon_B, |\Delta|$ .

## REFERENCES

- 
- [1] A. Peres, *Quantum Theory: Concepts and Methods*, (Kluwer Academic Publishers, The Netherlands, 1995).
- [2] C. H. Bennett, D. P. DiVincenzo, J. A. Smolin, W. K. Wootters, Phys. Rev. A **54**, 3824 (1996).
- [3] R. F. Werner, Phys. Rev. A **40**, 4277 (1989).
- [4] M. Horodecki, P. Horodecki, R. Horodecki, *Quantum Information - Basic Concepts and Experiments*, (Eds. G. Alber, M. Weiner, in print Springer, Berlin, 2000).
- [5] M. A. Nielsen and I. L. Chuang, *Quantum Computation and Quantum Information*, (Cambridge University Press, Cambridge, England, 2000).
- [6] J. Schliemann, J. I. Cirac, M. Kus, M. Lewenstein and D. Loss, Phys. Rev. A **64**, 022303 (2001).
- [7] J. Schliemann, D. Loss and A. H. MacDonald, Phys. Rev. B **63**, 085311 (2001).
- [8] K. Eckert, J. Schliemann, D. Bru, M. Lewenstein, Annals of Physics, **299**, 88 (2002).
- [9] P. Zanardi, Phys. Rev. Lett. **87**, 077901 (2001).
- [10] P. Zanardi, Phys. Rev. A **65**, 042101 (2002).
- [11] H. M. Wiseman and John A. Vaccaro, Phys. Rev. Lett. **91**, 097902 (2003).
- [12] M. R. Dowling, A. C. Doherty and H. M. Wiseman, Phys. Rev. A **73**, 052323 (2006).
- [13] L. Amico, R. Fazio, A. Osterloh and V. Vedral, Rev. Mod. Phys. **80** (2008).
- [14] A. P. Majtey, P. A. Bouvrie, A. Valdes-Hernandez and A. R. Plastino, Phys. Rev. A **93**, 032335 (2016).
- [15] M. Di Tullio, N. Gigena, and R. Rossignoli Phys. Rev. A **97**, 062109(2018).
- [16] G. Compagno, A. Castellini, R. L. Franco, Phil. Trans. R. Soc. A **376**, 20170317 (2018).
- [17] S. J. van Enk, Phys. Rev. A **67**, 022303 (2003).
- [18] F. Benatti, R. Floreanini, U. Marzolino, Phys. Rev. A **89**, 032326 (2014).
- [19] X.M. Puspup, K.H. Villegas, F.N.C. Paraan, Phys. Rev. B **90**, 155123 (2014).
- [20] D. Loss, and D. P. DiVincenzo, Phys. Rev. A **57** 120 (1998).
- [21] R. Hanson, R., L. P. Kouwenhoven, J. R. Petta, S. Tarucha, and L. M. K. Vandersypen, Rev. Mod. Phys. **79** 1217 (2007).
- [22] I. Buluta, S. Ashhab and F. Nori, Rep. Prog. Phys. **74** 104401(2011).
- [23] H. S. Borges, L. Sanz, J. M. Villas-Boas, O. O. Diniz Neto, and A. M. Alcalde, Phys. Rev. B **85**, 115425 (2012).
- [24] C. Carlson, D. Dalacu, Ch. Gustin, S. Haffouz, Xi. Wu, J. Lapointe, R. L. Williams, Ph. J. Poole, and S. Hughes, Phys. Rev. B **99**, 085311(2019).
- [25] M. Bayer, P. Hawrylak, K. Hinzer, S. Fafard, M. Korkusinski, Z. R. Wasilewski, O. Stern, and A. Forchel, Science **291**, 451 (2001).
- [26] R. Temirov, M. F. B. Green, N. Friedrich, Ph. Leinen, T. Esat, P. Chmielniak, S. Sarwar, J. Rawson, P. Kgerler, Ch. Wagner, M. Rohlfing, and F. S. Tautz, Phys. Rev. Lett. **120**, 206801(2018).
- [27] P. A. Oliveiraa, L. Sanza, Annals of Physics **356**, 244 (2015).
- [28] D. P. Daroca, P. Roura-Bas, and A. A. Aligia, Phys. Rev. B **97**, 165433 (2018).
- [29] A. S. Brackera, M. Scheibner, M. F. Doty, E. A. Stinaff, I. V. Ponomarev, J. C. Kim, L. J. Whitman, T. L. Reinecke, and D. Gammon, Appl. Phys. Lett. **89**, 233110 (2006).
- [30] C. Jennings and M. Scheibner, Phys. Rev. B **93**, 115311 (2016).
- [31] D. Malz and A. Nunnenkamp, Phys. Rev. B **97**, 165308 (2018).
- [32] G. Tang, L. Zhang and J. Wang, Phys. Rev. B **97**, 224311 (2018).
- [33] C. Song, K. Xu, W. Liu, Ch.-p. Yang, Sh.-B. Zheng, H. Deng, Q. Xie, K. Huang, Q. Guo, L. Zhang, P. Zhang, D. Xu, D. Zheng, X. Zhu, H. Wang, Y.-A. Chen, C.-Y. Lu, S. Han, and J.-W. Pan, Phys. Rev. Lett. **119** 180511 (2017).
- [34] C. Dickel, J. J. Wesdorp, N. K. Langford, S. Peiter, R. Sagastizabal, A. Bruno, B. Criger, F. Motzoi, and L. Di-Carlo, Phys. Rev. B **97** 064508 (2018).
- [35] Y. Wang, Y. Li, Z. Yin, B. Zeng, arXiv:1801.03782
- [36] Ch. Yang, Q. Su, Sh. Zheng, F. Nori, New J. Phys. **18** 013025 (2016).
- [37] D. J. Egger, M. Ganzhorn, G. Salis, A. Fuhrer, P. Mller, P.Kl. Barkoutsos, N. Moll, I. Tavernelli, and S. Filipp, Phys. Rev. Applied **11**, 014017(2019).
- [38] C. F. Roos, M. Riebe, H. Hffner, W. Hnsel, J. Benhelm, G. P. T. Lancaster, C. Becher, F. Schmidt-Kaler, R. Blatt, Science **304** 1478 (2004).
- [39] M. Riebe, H. Hffner, C. F. Roos, W. Hnsel, J. Benhelm, G. P. T. Lancaster, T. W. Krber, C. Becher, F. Schmidt-Kaler, D. F. V. James and R. Blatt, Nature **429** 734 (2004).
- [40] M. D. Barrett, J. Chiaverini, T. Schaetz, J. Britton, W.

- M. Itano, J. D. Jost, E. Knill, C. Langer, D. Leibfried, R. Ozeri and D. J. Wineland, *Nature* **429** 737 (2004).
- [41] J. Majer, J. M. Chow, J. M. Gambetta, J. Koch, B. R. Johnson, J. A. Schreier, L. Frunzio, D. I. Schuster, A. A. Houck, A. Wallraff, A. Blais, M. H. Devoret, S. M. Girvin and R. J. Schoelkopf, *Nature* **449** 443 (2007).
- [42] A. A. Houck, D. I. Schuster, J. M. Gambetta, J. A. Schreier, B. R. Johnson, J. M. Chow, L. Frunzio, J. Majer, M. H. Devoret, S. M. Girvin and R. J. Schoelkopf, *Nature* **449** 328 (2007).
- [43] D. I. Schuster, A. A. Houck, J. A. Schreier, A. Wallraff, J. M. Gambetta, A. Blais, L. Frunzio, J. Majer, B. Johnson, M. H. Devoret, S. M. Girvin and R. J. Schoelkopf, *Nature* **445** 515 (2007).
- [44] J. M. Martinis, S. Nam, J. Aumentado, and C. Urbina, *Phys. Rev. Lett.* **89** 117901 (2002).
- [45] J. R. Friedman, V. Patel, W. Chen, S. K. Tolpygo, and J. E. Lukens, *Nature* **406** 43 (2000).
- [46] C. H. van der Wal, A. C. ter Haar, F. K. Wilhelm, R. N. Schouten, C. J. Harmans, T. P. Orlando, S. Lloyd and J. E. Mooij, *Science* **290** 773 (2000).
- [47] Y. Yang, S. N. Coppersmith and M. Friesen, *npj Quantum Inf.* **5**, 12 (2019).
- [48] Y. Nakamura, Yu. A. Pashkin, and J. S. Tsai, *Nature* **398** 786 (1999).
- [49] J. R. Johansson, G. Johansson, and F. Nori, *Phys. Rev. A* **90** 053833 (2014).
- [50] M. Stern, G. Catelani, Y. Kubo, C. Grezes, A. Bienfait, D. Vion, D. Esteve, and P. Bertet *Phys. Rev. Lett.* **113** 123601 (2014).
- [51] Sheng-li Ma, Ji-kun Xie, Xin-ke Li, and Fu-li Li, *Phys. Rev. A* **99**, 042317(2019).
- [52] A. D. OConnell, M. Hofheinz, M. Ansmann, R. C. Bialczak, M. Lenander, Erik Lucero, M. Neeley, D. Sank, H. Wang, M. Weides, J. Wenner, John M. Martinis and A. N. Cleland, *Nature* **464** 697 (2010).
- [53] G. M. Reuther, D. Zueco, F. Deppe, E. Hoffmann, E. P. Menzel, T. Weil, M. Mariani, S. Kohler, A. Marx, E. Solano, R. Gross, and P. Hnggi, *Phys. Rev. B* **81** 144510 (2010).
- [54] J. Gambetta, A. Blais, M. Boissonneault, A. A. Houck, D. I. Schuster and S. M. Girvin, *Phys. Rev A* **77** 012112 (2008).
- [55] A. Blais, J. Gambetta, A. Wallraff, D. I. Schuster, S. M. Girvin, M. H. Devoret, and R. J. Schoelkopf, *Phys. Rev. A* **75** 032329 (2007).
- [56] J. P. Santos and F. L. Semio, *Phys. Rev. A* **89** 022128 (2014).
- [57] M. Woldeyohannes and S. John, *Phys. Rev. A* **60** 5046 (1999).
- [58] M. A. Reed, C. Zhou, C. J. Muller, T. P. Burgin and J. M. Tour, *Science* **278** 252 (1997).
- [59] H. Park, J. Park, A. K. L. Lim, E. H. Anderson, A. P. Alivisatos and P. L. McEuen, *Nature* **407** 57 (2000).
- [60] T. Dadoosh, Y. Gordin, R. Krahn, I. Khivrich, D. Mahalu, V. Frydman, J. Sperling, A. Yacoby and I. Bar-Joseph, *Nature* **436** 677 (2005).
- [61] C. A. Stafford and N. S. Wingreen, *Phys. Rev. Lett.* **76** 1916 (1996).
- [62] A. Nitzan and M. A. Ratner, *Nature* **300** 1384 (2003).
- [63] R. H. M. Smit, Y. Noat, C. Untied, N. D. Lang, M. C. van Hermert and J. M. van Ruitenbeek, *Nature* **419** 906 (2002).
- [64] A. Martin-Rodero, A. Levy Yeyati, *Adv. Phys.* **60**, 899 (2011).
- [65] M. G. Pala, M. Governale and J. Knig, *New J. Phys.* **10** 099801 (2008).
- [66] D. S. Kosov, T. Prosen and B. Zunkovi, *J. Phys.: Condens. Matter* **25** 075702 (2013).
- [67] S. P. Faller, A. Donarini and M. Grifoni, *Phys. Rev. B* **87** 155439 (2013).
- [68] E. Afsaneh and H. Yavari, *Few-Body Syst* **55** 159 (2014).
- [69] A. Jovchev and F. B. Anders, *Phys. Rev. B* **87**, 195112(2013).
- [70] A. Khedri, V. Meden, and T. A. Costi, *Phys. Rev. B* **96**, 195156(2017).
- [71] D. V. Averin and K. K. Likharev, *Physics* **62**, 345 (1986).
- [72] C. W. J. Beenakker and A. A. M. Staring, *Phys. Rev. B* **46**, 9667 (1992).
- [73] P. G. De Gennes, *Superconductivity Of Metals And Alloys*, (Westview Press, 1999).
- [74] M. Tinkham, *Introduction to Superconductivity*, (McGraw-Hill, New York, 1996).
- [75] G. D. Mahan, *Many-Particle Physics*, (Springer Science and Business Media, 1990).
- [76] U. Harbola, M. Esposito and S. Mukamel, *Phys. Rev. B* **74** 235309 (2006).
- [77] S. Hill, and W. K. Wootters, *Phys. Rev. Lett.* **78** 5022 (1997).
- [78] W. K. Wootters, *Phys. Rev. Lett.* **80** 2245 (1998).
- [79] P. Rungta, V. Buzek, C. M. Caves, M. Hillery and G. J. Milburn, *Phys. Rev. A* **64**, 042315 (2001).
- [80] J-H Jiang, M. Kulkarni, D. Segal, and Y. Imry, *Phys. Rev. B* **92**, 045309 (2015).
- [81] J. B. Ketterson, S. N. Song, *Superconductivity*, (Cambridge University Press, 1999).
- [82] H. P. Breuer and F. Petruccione, *The Theory of Open Quantum Systems*, (Oxford University Press, 2002).
- [83] T. A. Baart, N. Jovanovic, C. Reichl, W. Wegscheider and L. M. K. Vandersypen, *Appl. Phys. Lett.* **109** 043101 (2016).
- [84] P. Harvey-Collard, N. T. Jacobson, M. Rudolph, J. Dominguez, G. A. Ten Eyck, J. R. Wendt, T. Pluym, J. K. Gamble, M. P. Lilly, M. Pioro-Ladriare and M. S. Carroll, *Nat. Commun.* **8** 1029 (2017).